

Supporting Information

Gas storage within nanoporous material encapsulated by ice

**Jia Ming Goh^a, Zhi Yu^a, Ali Zavabeti^a, Shuangmin Shi^b, Yalou Guo^c, Jianan He^a, Jianing Yang^a,
Lei Dong^a, Paul A. Webley^c, Amanda Vera Ellis^a, Gang Kevin Li^{*a}**

^a Department of Chemical Engineering, The University of Melbourne, Parkville, Victoria 3010, Australia

^b Department of Infrastructure Engineering, The University of Melbourne, Parkville, Victoria 3010, Australia

^c Department of Chemical & Biological Engineering, Monash University, Clayton, Victoria 3800, Australia

Supplementary Note 1. Free Space Measurement

To determine the free space of the autoclave, its internal volume was first being measured. The autoclave was connected to a vacuum pump via a valve where the pump was turned on to allow for gas evacuation. After a few minutes, the valve was closed then the vacuum pump was turned off. The weight of the empty autoclave was measured as 862.9 g. The autoclave was immersed into a large beaker of water with the water level above the opening of the autoclave. The valve was opened to allow for water filling into the autoclave. With the valve closed, the autoclave was removed from the beaker and its surface was wiped dry, making sure there is no excess water. The weight of the autoclave with water was measured as 908 g. Difference between the two weights gives the mass of the water, which is equivalent to a volume of 45.1 mL.

Supplementary Note 2. Methodology for quantifying gas released from adsorption

In the gas storage cycle experiments, the gas collected from the autoclave after the ice melts includes four components, as detailed in the main manuscript. To assess the success of gas storage within ice-encapsulated silicalite-1, we compared the adsorption component of the gas released from the warmed-up autoclave with the values measured for dry samples. Calculations are required to isolate the portion of the gas attributed to adsorption:

(a) Release of dissolved gas in the water

All atmospheric gases can dissolve in water, following Henry's law, which states that the amount of dissolved gas is proportional to its partial pressure and Henry's law constant. In a closed autoclave with water, gas dosed at room temperature will dissolve into the water. When the autoclave is sealed and cooled in a freezer, the internal pressure decreases as the temperature drops, affecting the amount of dissolved gas until the water freezes at around 0 °C. According to Gay-Lussac's Law ($P_1/T_1 = P_2/T_2$), if the gas is initially dosed at 35 bar at 20 °C, the pressure will decrease to approximately 32.6 bar as the temperature reaches 0 °C. The solubility data for nitrogen and methane under pressure in water, used for calculations in this study, are provided in Table S4. The amount of dissolved gas released is calculated by subtracting the amount of gas dissolved in water at ambient pressure and temperature from the amount dissolved at freezing pressure and temperature.

(b) Expansion of the air in the free space due to temperature change

After leaving the autoclave in the freezer overnight, the valve was opened to relieve the internal pressure, allowing the free space within the autoclave to be filled with air at ambient pressure and freezing temperature. When the autoclave was brought back to room temperature, the air in the free space expanded according to Charles's Law ($V_1/T_1 = V_2/T_2$). To accurately quantify this expanded air, it is essential to know the volume of the free space. The internal volume of

the autoclave was measured to be 45.1 mL. To calculate the free space volume, we subtracted the volumes occupied by the water, the sample, the aluminium foil holding the sample, and the plastic tube supporting the sample. The volumes of these substances were determined by measuring their masses and dividing by their respective densities (Table S5).

(c) Vapour pressure of water

As the autoclave warmed up to room temperature, changes in the vapour pressure of water were anticipated. It was postulated that water vapour within the autoclave achieved equilibrium with its liquid counterpart throughout the gas collection interval. This parameter was quantified employing the ideal gas law expressed as $P_iV = nRT$, where P_i denotes the partial pressure of water vapour, V signifies the internal free space volume of the autoclave, and n indicates the moles of water vapour present. The vapour pressure of water at $-20\text{ }^\circ\text{C}$ was assumed to be effectively zero, whereas at $20\text{ }^\circ\text{C}$, it was documented at 2.3388 kPa.¹ The calculation of the internal free space volume was conducted based on methodologies outlined in prior sections.

Upon determining the values for these three components, they were subsequently subtracted from the total gas volume. This subtraction was performed to isolate and quantify the volume of gas adsorbed and desorbed from the internal pores of the ice-encapsulated silicalite-1 particles.

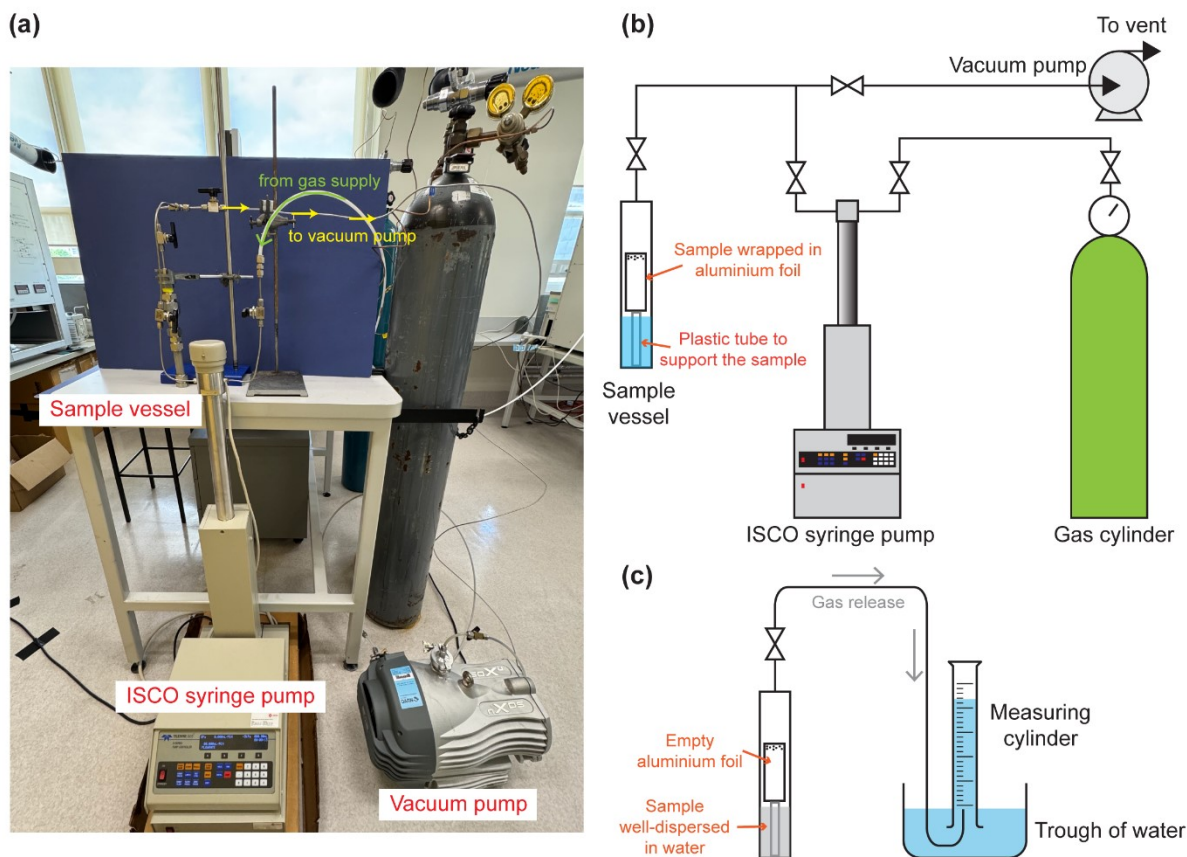


Figure S1. (a) Apparatus set up for controlled gas dosage into the sample vessel containing the silicalite-1 samples. (b) Schematic of the apparatus set up. (c) Water displacement setup to quantify the amount of gas released from the warmed-up sample vessel.

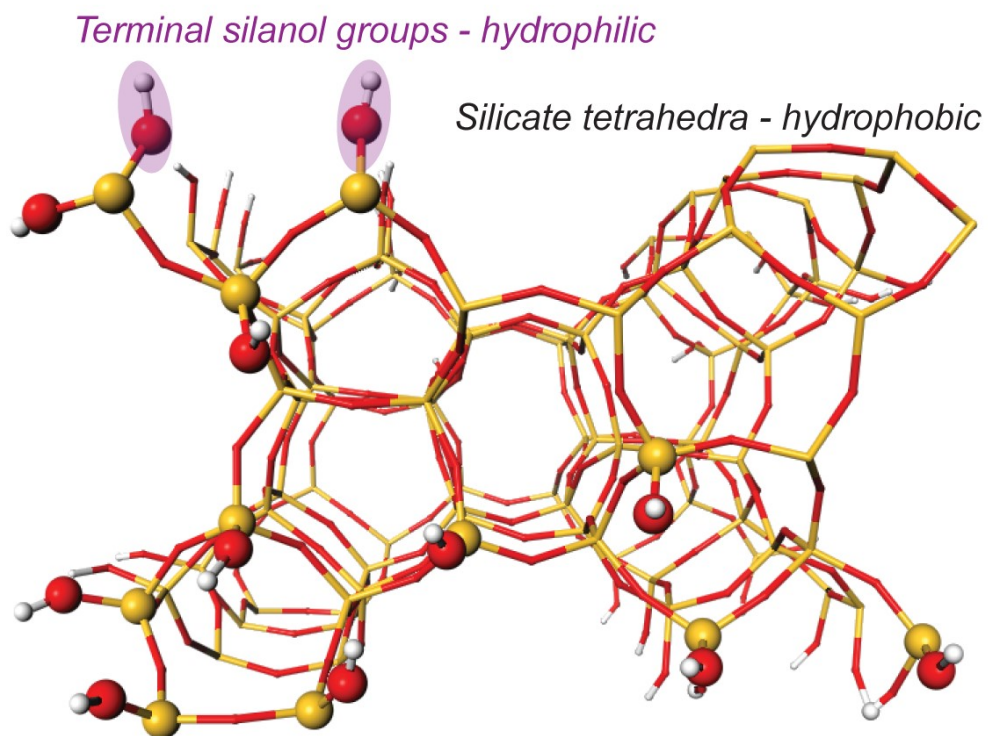


Figure S2. Crystal structure of silicalite-1 showing the hydrophobic silicate tetrahedra framework and hydrophilic terminal silanol groups.

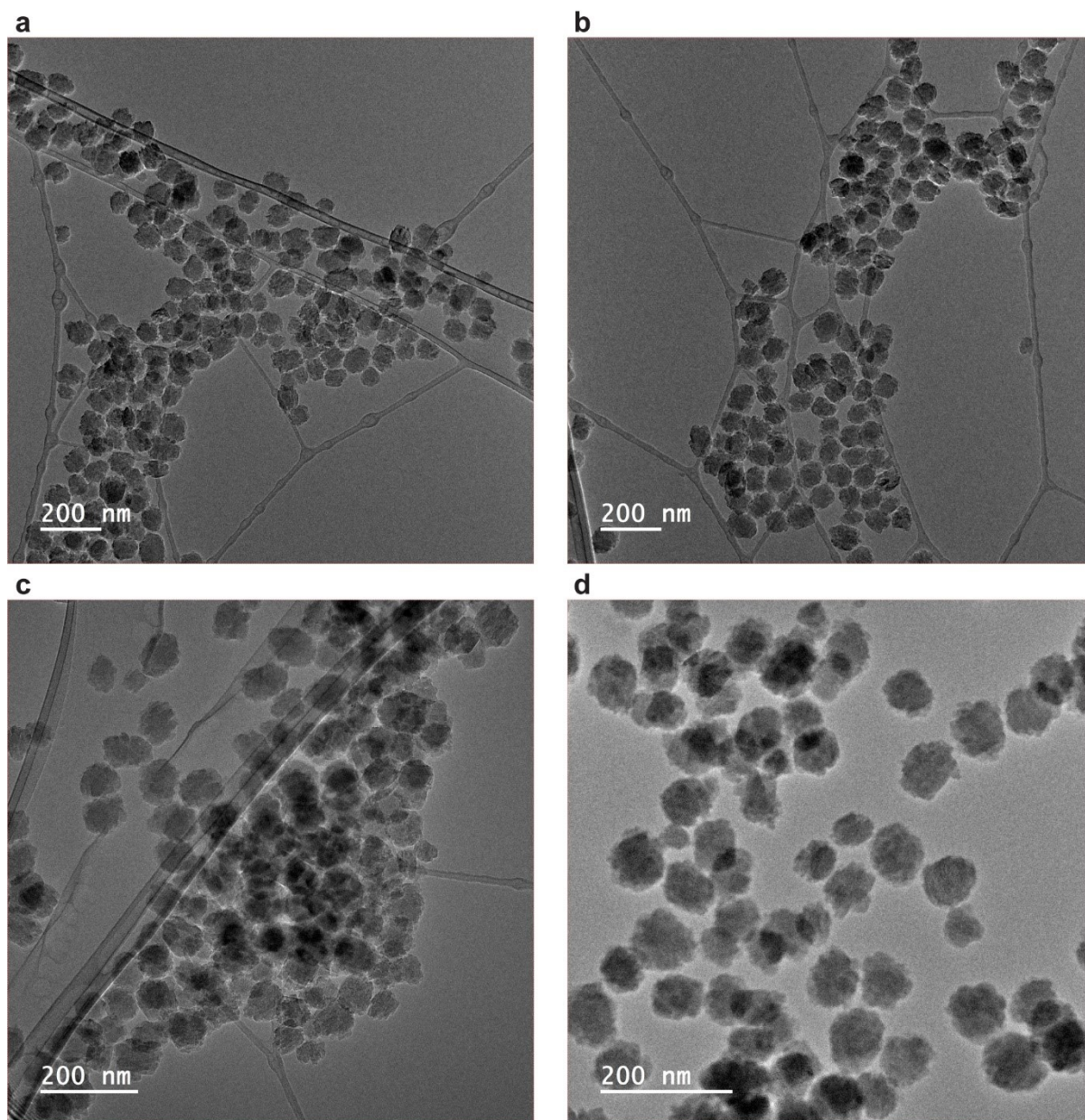


Figure S3. Low-resolution TEM images of the synthesized silicalite-1 nanocrystals.

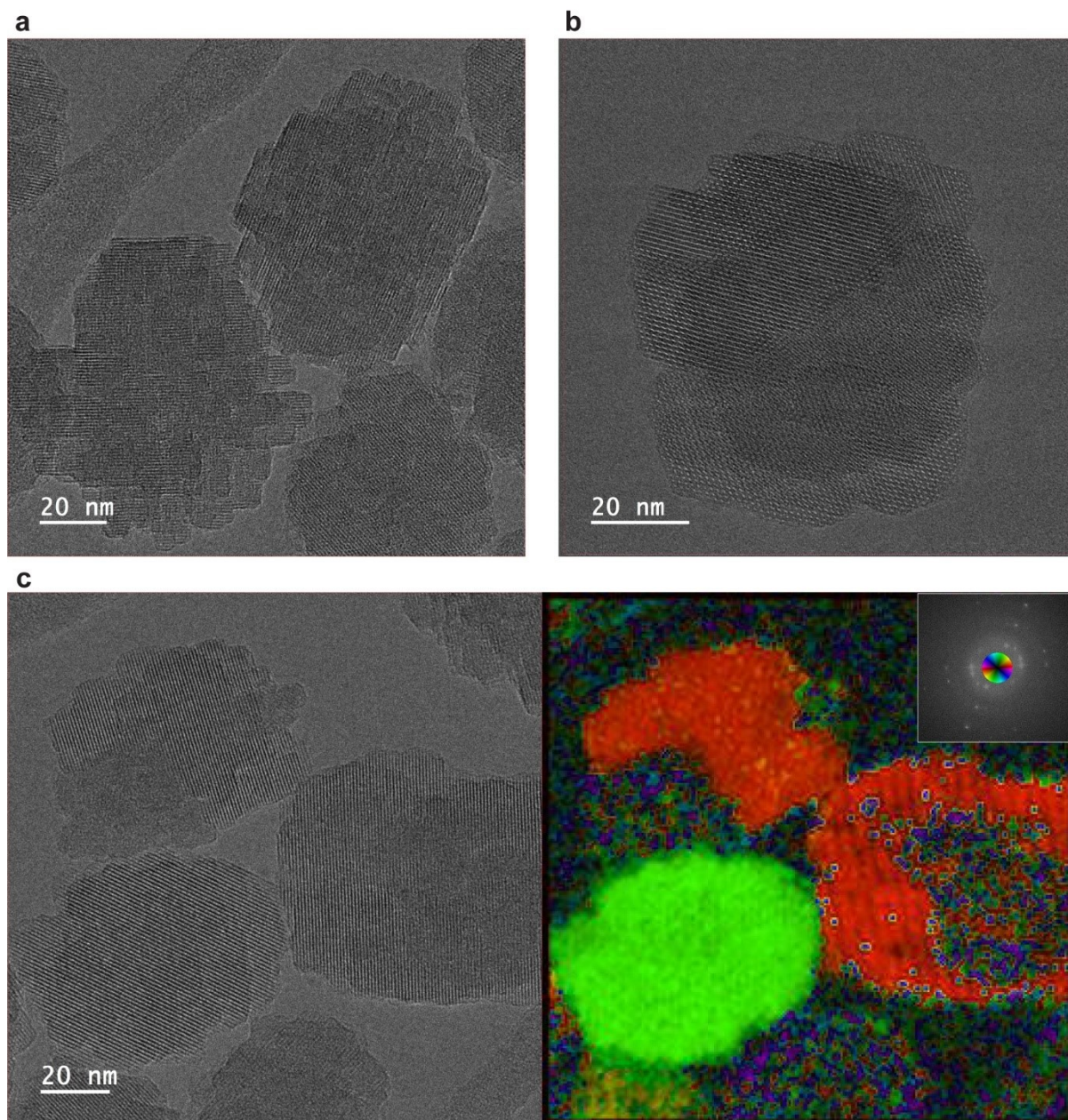


Figure S4. (a-b) HRTEM images of the synthesized silicalite-1 nanocrystals. (c) HRTEM image (left) of the nanocrystals and corresponding orientation map (right), with colours indicating different crystallographic orientations. Inset: Colour-coded SAED pattern correlating with the orientations in the map.

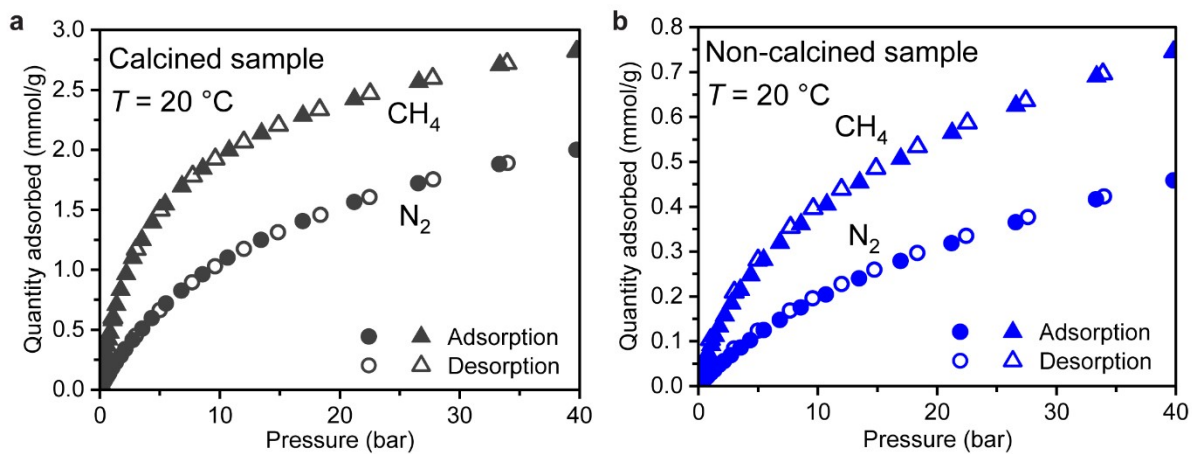


Figure S5. N₂ and CH₄ adsorptions of (a) calcined and (b) non-calcined silicalite-1 samples.

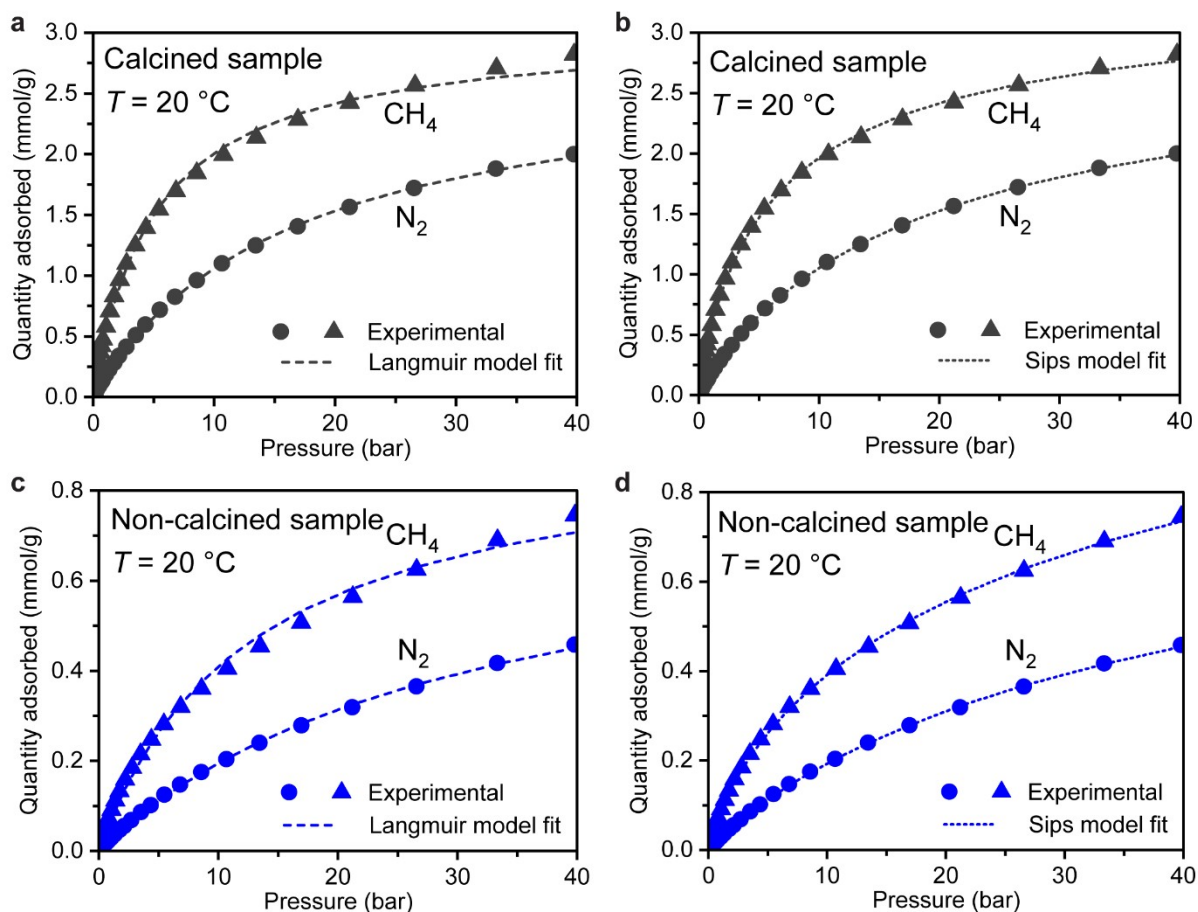


Figure S6. N_2 and CH_4 adsorption isotherms of calcined (a, b) and non-calcined (c, d) silicalite-1 samples fitted by Langmuir (a, c) and Sips (b, d) models. The figures demonstrate that the Sips model provides a superior fit to the experimental data, particularly for CH_4 adsorption at higher pressures. The model parameters and comparison of r^2 values are presented in Table S2.

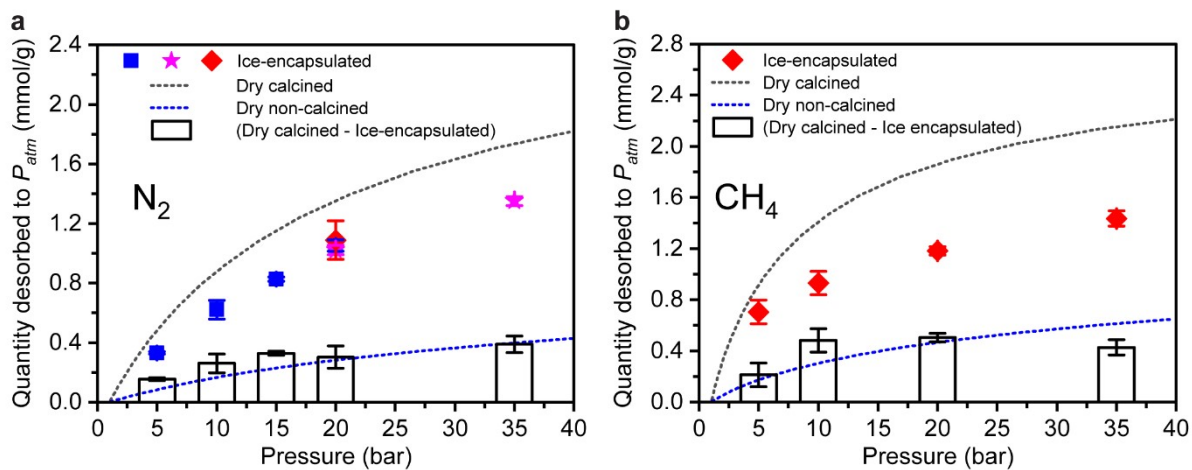


Figure S7. Comparison of the amounts of N_2 (a) and CH_4 (b) desorbed to atmospheric pressure at 20 °C between the non-calcined sample and the calculated isotherm, derived from the difference in desorbed amounts between the dry calcined and H_2O -encapsulated samples.

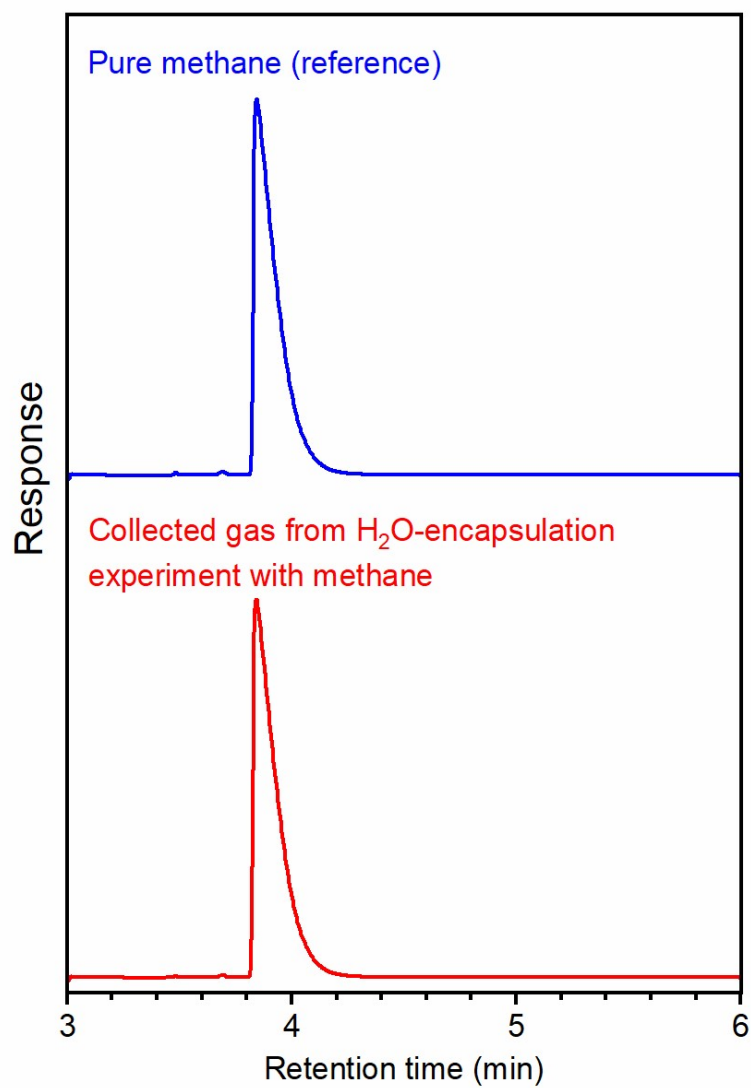


Figure S8. Gas chromatography results comparing pure CH₄ (sample reference) with the gas collected from the warmed-up autoclave containing H₂O-encapsulated silicalite-1 with CH₄.

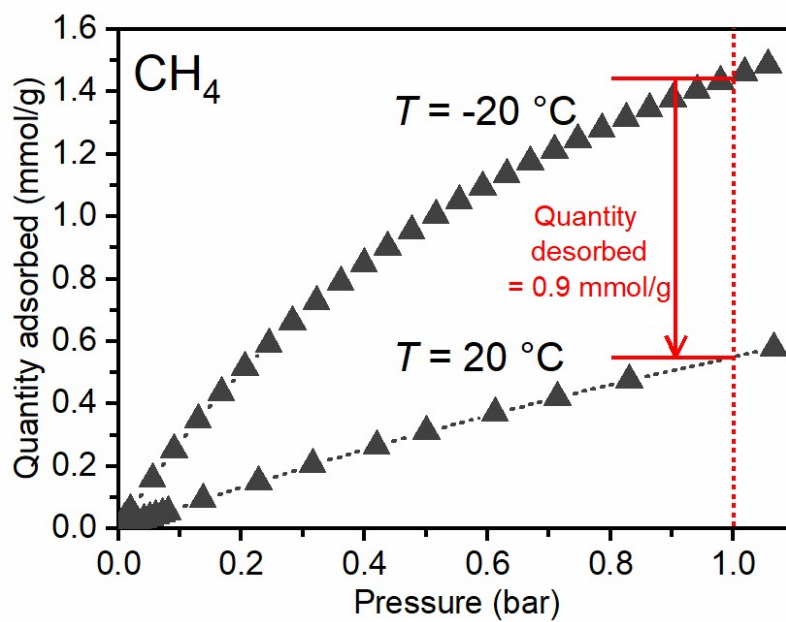


Figure S9. Comparison of CH₄ adsorption quantities of calcined silicalite-1 sample at 20 °C and -20 °C .

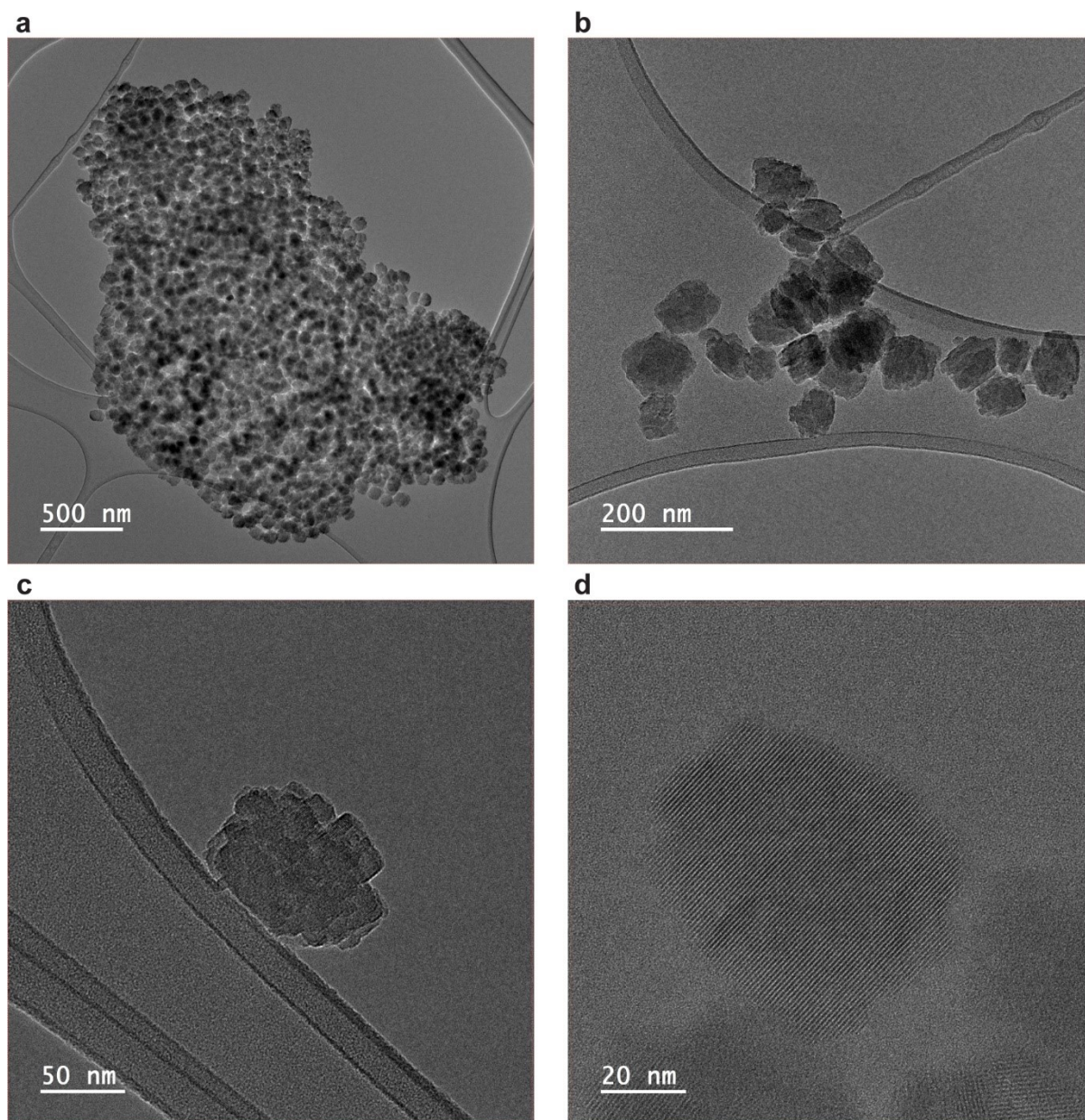


Figure S10. (a-c) Low-magnification TEM images and (d) HRTEM image of the used silicalite-1 sample.

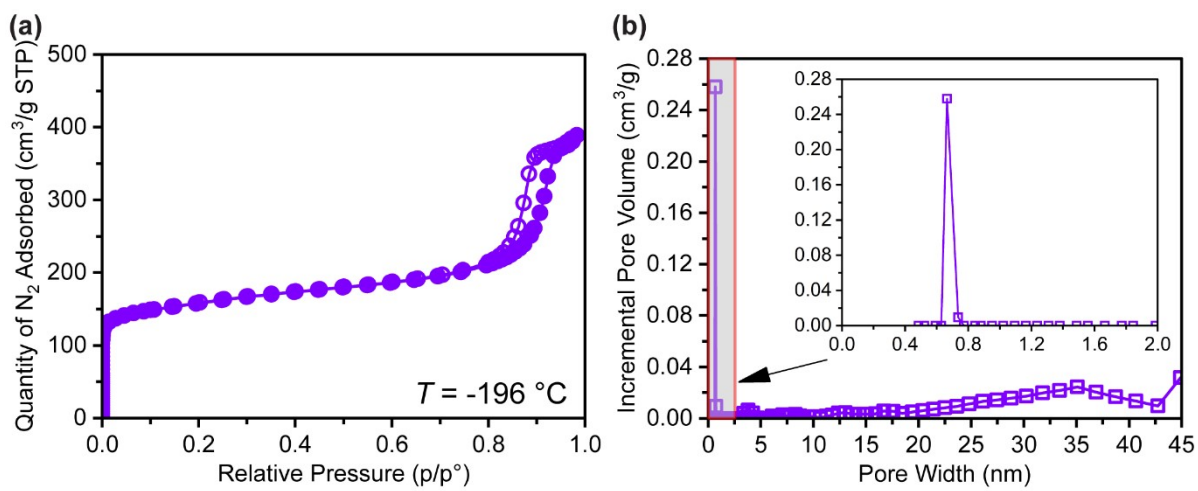


Figure S11. (a) N_2 adsorption at $-196\text{ }^{\circ}\text{C}$ and (b) NLDFT pore size distribution of the silicalite-1 samples after 22 gas storage cycles.

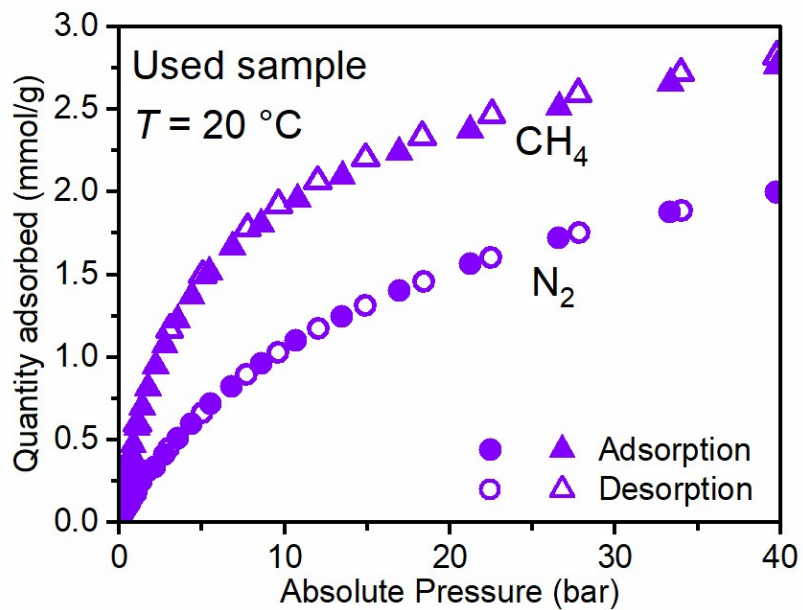


Figure S12. N₂ and CH₄ adsorptions of the silicalite-1 samples after 22 gas storage cycles.

Table S1. Summary of BET surface areas and pore volumes for the silicalite-1 samples obtained from N₂ adsorption isotherms at -196 °C.

Condition	BET surface area (m²/g)	Micropore volume (mL/g)	Mesopore volume (mL/g)	Total pore volume (mL/g)
Fresh	498.2	0.275	0.351	0.626
After 22 gas storage cycles	499.6	0.271	0.343	0.614

Table S2. Sips and Langmuir fitting parameters for N₂ and CH₄ adsorption on different silicalite-1 samples. Sips:² $q = \frac{q_m(KP)^n}{1 + (KP)^n}$; Langmuir:³ $q = \frac{q_m KP}{1 + KP}$, where q_m is the saturation loading, p is the partial pressure of the adsorbate in the gas phase, K is the Langmuir affinity parameter, and n is the Freundlich exponent. It should be noted that for the H₂O-encapsulated sample, the data points are the amounts desorbed to atmospheric pressure. In this case, the pressure term in the Sips model equation is subtracted by 1.01325 bar.

Condition	Gas	Sips				Langmuir		
		q_m (mmol/g)	K (bar ⁿ)	n	r^2	q_m (mmol/g)	K (bar ⁻¹)	r^2
Dry non-calcined	N ₂	0.958	0.0225	0.9228	0.9999	0.803	0.0320	0.9995
	CH ₄	1.368	0.0306	0.7692	0.9995	0.935	0.0781	0.9954
Dry calcined	N ₂	2.947	0.0540	0.9554	1.0000	2.784	0.0614	0.9998
	CH ₄	3.364	0.1491	0.8585	0.9994	3.034	0.1956	0.9977
H ₂ O-encapsulated (desorbed to P_{atm})	N ₂	2.196	0.0540	0.9392	0.9989	-	-	-
	CH ₄	2.595	0.1491	0.6000	0.9980	-	-	-

Table S3. Summary of gas storage results at different experimental conditions.

Gas	Dosage pressure, P_d (bar)	Freezing temperature, T_f (°C)	Water-to- sample mass ratio, R_w	Average quantity desorbed to P_{atm} (mmol/g)
N ₂	5	-5	13	0.32
	10	-5	13	0.61
	15	-5	13	0.81
	20	-5	13	1.04
	20	-20	13	1.00
	20	-20	3	1.08
	35	-20	13	1.34
	35	-20	5	1.34
	35	-20	3	1.34
	35	-20	2	1.34
CH ₄	5	-20	3	0.70
	10	-20	3	0.92
	20	-20	3	1.17
	35	-20	3	1.42
	35	-20	2	1.21

Table S4. Solubility data for N₂ and CH₄ in water under different pressures and temperatures.

Dosage pressure, P_d at 20 °C (bar)	Freezing pressure, P_f at 0 °C (bar)	Gas	Solubility in water at P_f (cm ³ /g at 20 °C, 1 atm)	Ref.
1	-	N ₂	0.0160 ^a	4
5	4.7	N ₂	0.107	4
10	9.3	N ₂	0.196	4
15	14.0	N ₂	0.266	4
20	18.6	N ₂	0.348	4
35	32.6	N ₂	0.586	4
1	-	CH ₄	0.0399 ^a	5
5	4.7	CH ₄	0.256	5
10	9.3	CH ₄	0.507	5
20	18.6	CH ₄	1.008	5
35	32.6	CH ₄	1.413 ^b	5

^a Gas solubility in water at dosage pressure, P_d at 20 °C.

^b The solubility of methane at 26.17 bar and 0 °C – the equilibrium pressure for methane hydrate formation – is used, as pressures above this point lead to hydrate formation, limiting further dissolution of methane in water even at higher pressures.

Table S5. Densities of substances that occupy volume within the autoclave.

Substance	Density (g/mL)
Water	1.00
Degassed silicalite-1	1.84 ^a
Aluminium foil	2.71
Plastic tube	0.93

^a crystallographic density⁶

References

1. D. R. Lide, *CRC handbook of chemistry and physics*, CRC press, 2004.
2. R. Sips, *J. Chem. Phys.*, 1948, **16**, 490-495.
3. I. Langmuir, *J. Am. Chem. Soc.*, 1918, **40**, 1361-1403.
4. V. I. Baranenko, V. S. Sysoev, L. N. Fal'kovskii, V. S. Kirov, A. I. Piontkovskii and A. N. Musienko, *At. Energy*, 1990, **68**, 162-165.
5. Z. Duan and S. Mao, *Geochim. Cosmochim. Acta*, 2006, **70**, 3369-3386.
6. Database of Disordered Zeolite Structures, <http://www.iza-structure.org/databases/>, (accessed June 2024).